RSC Advances

PAPER

View Article Online
View Journal | View Issue

Cite this: *RSC Adv.*, 2023, **13**, 29477

Mitochondria-targeting EGCG derivatives protect H9c2 cardiomyocytes from H_2O_2-induced apoptosis: design, synthesis and biological evaluation†

Revathy Sahadevan,‡[a] Anupama Binoy,‡[a] Irene Shajan[a] and Sushabhan Sadhukhan *[ab]

Pathologies related to cardiovascular diseases mostly emerge as a result of oxidative stress buildup in cardiomyocytes. The heavy load of mitochondrial oxidative phosphorylation in cardiac tissues corresponds to a surge in oxidative stress leading to mitochondrial dysfunction and cellular apoptosis. Thus, scavenging the reactive oxygen species (ROS) linked to mitochondria can significantly improve cardio-protection. Epigallocatechin-3-gallate (EGCG), the major polyphenol found in green tea has been extensively studied for its profound health-beneficial activities. Herein, we designed and synthesized a series of mitochondrial-targeting EGCG derivatives, namely MitoEGCG$_n$ (n = 4, 6, 8) by incorporating triphenylphosphonium ion onto it using different linkers. MitoEGCG$_n$ were found to be non-toxic to H9c2 rat cardiomyocyte cells even at higher doses in comparison to its parent molecule EGCG. Interestingly, MitoEGCG$_4$ and MitoEGCG$_6$ protected the H9c2 cardiomyocyte cells from the oxidative damage induced by H_2O_2 whereas EGCG was found to be toxic and ineffective in protecting the cells from H_2O_2 damage. MitoEGCG$_4$ and MitoEGCG$_6$ also protected the cells from the H_2O_2-induced disruption of mitochondrial membrane potential as well as activation of apoptosis as revealed by pro-caspase 3 expression profile, DNA fragmentation assay, and AO/EtBr staining. Taken together, our study shows that the mitochondria targeting EGCG derivatives were able to effectively combat the H_2O_2-induced oxidative stress in H9c2 cardiomyocytes. They eventually augmented the mitochondrial health of cardiomyocytes by maintaining the mitochondrial function and attenuating apoptosis. Overall, MitoEGCG$_4$ and MitoEGCG$_6$ could provision a cardioprotective role to H9c2 cardiomyocytes at the time of oxidative insults related to mitochondrial dysfunction-associated injuries.

Received 7th July 2023
Accepted 2nd October 2023

DOI: 10.1039/d3ra04527g

rsc.li/rsc-advances

1. Introduction

Cardiovascular diseases are counted among the leading reasons for a very large number of human deaths worldwide.[1] The World Health Organization (WHO) has predicted that the mortality rate due to cardiovascular related diseases might elevate to 25 million by 2030.[2,3] The pathological progression of cardiac damage is mostly linked to the elevated degree of oxidative stress in cells, which can be brought on by a number of factors including fat accumulation, a sedentary lifestyle, consuming food high in saturated fat and sodium ion, *etc.* These damages are multifaceted as oxidative stress results in the accumulation of free radicals which harms several biomolecules like DNA, lipids and proteins.[4,5] It also plays a central role in activating a redox-regulated signaling cascade which can culminate into mitochondrial-associated cell death.[6,7] Mitochondria are considered as the powerhouse of the cell. The production of ATP in the mitochondria through oxidative phosphorylation intrinsically produces ROS and this makes the mitochondrion as the primary source for intracellular ROS. Due to the higher aerobic metabolism in heart tissues, mitochondria are highly susceptible to oxidative damage leading to mitochondrial dysfunction which can ultimately initiate intrinsic apoptotic pathways.[8,9] Hence, the development of therapeutic strategies to overcome the mitochondrial dysfunction-associated injuries to heart tissues caused by ROS can prove helpful in installing a check in the progression of cardiovascular diseases.

Green tea has gained global attention in recent times due to its remarkable antioxidant, anti-carcinogenic, cardioprotective, neuroprotective and anti-inflammatory properties.[10–13] (−)-Epigallocatechin-3-gallate (EGCG) is the most abundant

[a]*Department of Chemistry, Indian Institute of Technology Palakkad, Kerala 678 623, India. E-mail: sushabhan@iitpkd.ac.in*

[b]*Physical & Chemical Biology Laboratory, and Department of Biological Sciences & Engineering, Indian Institute of Technology Palakkad, Kerala 678 623, India*

† Electronic supplementary information (ESI) available. See DOI: https://doi.org/10.1039/d3ra04527g

‡ Equal contribution.

polyphenol in green tea accounting for about 50–75% of the catechins and is responsible for the majority of health benefits attributed to green tea. It has also been classified as 'Generally Recognized as Safe (GRAS)' for its health beneficial effects by the United States Food and Drug Administration (FDA) and European Food Safety Authority (EFSA). EGCG is well studied for its antioxidant property which is due to the presence of the eight phenolic hydrogens. Its structure allows electron delocalization, conferring it with radical scavenging activity. It is known to react with ROS such as superoxide radical ($O_2^{\bullet -}$), singlet oxygen ($^1O_2$), hydroxyl radical ($OH^{\bullet}$), peroxyl radical ($ROO^{\bullet}$), nitric oxide (NO), *etc.*[14] However, the therapeutic effect of EGCG is hampered by its poor systemic absorption after oral administration, poor gastrointestinal tract stability and pharmacokinetics, low bioavailability, first-pass metabolism, constrained membrane permeability across the intestine, and low accumulation in the related tissues.[15] In our recent report, we conducted a chemoproteomics-based protein profiling of EGCG in HeLa cells. The post-proteomics analysis provided insightful information on the molecular mechanism of action behind the plethoric biological activities exhibited by EGCG.[16] Previously, we have successfully demonstrated that an alkyl substitution at the 4″-position on the D-ring hydroxyl group can be explored to generate EGCG analogues with increased bioavailability and thus enhanced biological activity.[17,18] The characteristic resonance stabilization of the phenolate at the 4″-position provides scope for regioselective alkylation at this position.

Herein, we strategically designed mitochondria-targeting EGCG analogues (MitoEGCG$_n$) by conjugating EGCG with a triphenylphosphonium cation (TPP) through hydrophobic alkyl linkers. The linker serves a dual purpose: (i) an optimum distance between EGCG and TPP to avoid any potential steric hindrance and (ii) the required balance between the hydrophobicity and hydrophilicity to cross the mitochondrial membrane. TPP is a widely used lipophilic cation for mitochondrial targeting due to its positive charge which is delocalized throughout the aromatic rings making it membrane permeant.[19,20] Due to the large mitochondrial membrane potential (~120–180 mV, negative inside), MitoEGCG$_n$ can readily accumulate in the mitochondria and can exert its antioxidant activity to safeguard mitochondrial health from severe oxidative damages. Herein, we have used the H9c2 rat cardiomyocytes with H_2O_2-induced oxidative stress as a cardiac injury model for current investigation.[21,22] Even at high concentrations, MitoEGCG$_n$ (n = 4, 6 and 8) was found to be substantially less toxic than EGCG. The structural modifications on EGCG did not compromise on the biological activities exhibited by their mitochondrial analogues as shown by *in vitro* radical scavenging activity analysis. MitoEGCG$_4$ and MitoEGCG$_6$ both were able to reduce H_2O_2-induced cytotoxicity in rat cardiomyocytes in comparison to EGCG. The inhibition of the mitochondrial outer membrane potential (Ψ_m) reduction upon MitoEGCG$_n$ treatment demonstrates that those agents protected the cells from H_2O_2-induced oxidative mitochondrial damage brought on by ROS formation. Thus, our study provides a strategic model for developing mitochondria-targeting natural polyphenols as a cardioprotective agent during cardiovascular pathologies.

2. Materials and methods

2.1. Chemicals

EGCG was purchased from Biosynth Carbosynth, USA. Anhydrous NaOAc and triphenylphosphine were purchased from NICE Chemicals, India and Spectrochem, India, respectively. 3-(4,5-Dimethylthiazol-2-yl)-2,5-diphenyltetrazolium bromide (MTT), anhydrous Na_2SO_4, and $NaHCO_3$ were purchased from Sisco Research Laboratories (SRL), India. All solvents used were of reagent grades and used as purchased (NICE Chemicals, India) without any further purification. Amphotericin, tris buffer, sodium dodecyl sulphate (SDS), tween-20, Triton X 100, glycerol, glycine, Dulbecco's Modified Eagle Medium (DMEM), fetal bovine serum (FBS), antibiotics comprised of Penicillin and Streptomycin were purchased from HiMedia, India. H_2O_2, TMRE and DCFHDA dyes were purchased from Sigma-Aldrich, India. Anti-pro-caspase 3 and anti-rabbit IgG HRP-linked antibodies were procured from Cell Signaling Technology, USA.

2.2. Synthesis of MitoEGCG$_n$

MitoEGCG$_n$ derivatives were synthesized in three steps as described below.

2.2.1 Step 1: Synthesis of 1,*n*-dibromoalkane (where n = 4, 6, and 8). To a mixture of alkane-1,*n*-diol (11.47 mmol, 1 equiv.) in water (20 mL), hydrobromic acid (HBr) (172.14 mmol, 15 equiv.) was added. The mixture was stirred under reflux for 48 h. After the completion of the reaction, the dibromoalkane compounds were extracted with chloroform ($CHCl_3$) (20 mL × 3). The $CHCl_3$ layer was then neutralized by washing with saturated sodium bicarbonate ($NaHCO_3$) solution (20 mL × 2). The organic layer was dried by passing over anhydrous sodium sulphate (Na_2SO_4). The pale-yellow liquid dibromoalkane compounds were obtained by the evaporation of the solvent under reduced pressure. The obtained product was directly used for the next step without any purification.

2.2.2 Step 2: Synthesis of EGCG-C$_n$Br (where n = 4, 6, and 8). To a mixture of EGCG (0.45 mmol, 1 equiv.) in dry dimethylformamide (DMF) (2 mL), anhydrous sodium acetate (NaOAc) (1.31 mmol, 3 equiv.) and 1,*n*-dibromoalkane (2.25 mmol, 5 equiv.) was added one by one. The mixture was stirred for 2 h at 85 °C. The progress of the reaction was monitored by thin-layer chromatography (TLC). The reaction was quenched by the addition of H_2O (5 mL) and the desired compound was extracted with ethyl acetate (EA) (5 mL × 3). The EA layer was washed well with H_2O (5 mL × 3) to remove the DMF. The organic layer was dried by passing over anhydrous sodium sulphate (Na_2SO_4) and the crude compounds were obtained by the evaporation of the solvent under reduced pressure. The desired compounds, (EGCG-C$_n$Br) were purified by silica gel column chromatography (silica: 230–400 mesh size and solvent: 20% acetone–DCM).

2.2.3 Step 3: Synthesis of MitoEGCG$_n$ (where n = 4, 6, and 8). EGCG-C$_n$Br (0.16 mmol, 1 equiv.) obtained from the previous

step was dissolved in acetonitrile (50 mL) and the mixture was then treated with triphenylphosphine (TPP) (0.81 mmol, 5 equiv.). The reaction was allowed to stir for 36 h at 100 °C. The progress of the reaction was monitored by thin-layer chromatography (TLC). At the end of the reaction, the crude compounds were obtained by the evaporation of the solvent under reduced pressure. The desired compounds, MitoEGCG$_n$ were purified by silica gel column chromatography (silica: 230–400 mesh size and solvent: 20% methanol–EA) as pale brown solids.

2.3. Instruments used for the characterization of MitoEGCG$_n$ compounds

Shimadzu LC-MS-8045 instrument is used for the LC-MS (liquid chromatography-mass spectrometry) characterization of the MitoEGCG$_n$ compounds by utilizing the Sprite TARGA C18 column with dimensions 40 × 2.1 mm, 5 μm and monitored at 210 and 254 nm in positive mode of ionization for mass detection. ^{1}H NMR and ^{13}C NMR spectra were recorded in Bruker Ascend 400 NMR spectrometer.

2.4. Characterization of MitoEGCG$_n$

2.4.1 MitoEGCG$_4$. The compound was obtained with 59% yield and 99.2% purity. MS (ESI): m/z calculated for $C_{44}H_{40}O_{11}P^+$ = 775.23, observed = 775.20. ^{1}H NMR (400 MHz, DMSO-d$_6$): δ (ppm) = 7.89–7.73 (15H, m), 6.84 (2H, s), 6.43 (2H, s), 5.94 (1H, d, J = 2.24 Hz), 5.84 (1H, d, J = 2.24 Hz), 5.38 (1H, m), 4.97 (1H, m), 3.97 (2H, t, J = 5.88 Hz), 2.95 (1H, dd, J = 17.14 and 4.38 Hz), 2.66 (1H, d, J = 16.52 Hz), 1.82 (2H, m), 1.74 (2H, m), 1.29 (2H, m). ^{13}C NMR (100 MHz, DMSO-d$_6$): δ (ppm) = 164.95, 156.57, 156.50, 155.57, 150.68, 145.66, 138.51, 134.93, 133.51, 132.36, 130.22, 128.38, 124.25, 118.95, 118.10, 108.70, 105.45, 97.26, 95.55, 94.38, 76.34, 70.48, 68.47, 30.73, 28.39, 22.42, 13.93, 10.84.

2.4.2 MitoEGCG$_6$. The compound was obtained with 56% yield and 99.4% purity. MS (ESI): m/z calculated for $C_{46}H_{44}O_{11}P^+$ = 803.26, observed = 803.35. ^{1}H NMR (400 MHz, DMSO-d$_6$): δ (ppm) = 7.92–7.70 (15H, m), 6.81 (2H, s), 6.40 (2H, s), 5.93 (1H, d, J = 2.24 Hz), 5.82 (1H, d, J = 2.32 Hz), 5.37 (1H, m), 4.95 (1H, m), 3.87 (2H, t, J = 6.12 Hz), 2.93 (1H, dd, J = 16.68 and 4.14 Hz), 2.65 (1H, d, J = 16.68 Hz), 1.51 (6H, m), 1.37 (2H, m), 1.21 (2H, m). ^{13}C NMR (100 MHz, DMSO-d$_6$): δ (ppm) = 164.99, 156.58, 156.51, 155.59, 150.70, 145.71, 138.86, 134.90, 133.53, 132.42, 130.21, 128.49, 124.15, 119.01, 118.16, 108.69, 105.46, 97.28, 95.55, 94.37, 76.38, 71.59, 68.47, 48.63, 29.05, 24.44, 21.69, 20.40, 19.90.

2.4.3 MitoEGCG$_8$. The compound was obtained with 52% yield and 98.6% purity. MS (ESI): m/z calculated for $C_{48}H_{48}O_{11}P^+$ = 831.29, observed = 831.25. ^{1}H NMR (400 MHz, DMSO-d$_6$): δ (ppm) = 7.90–7.74 (15H, m), 6.84 (2H, s), 6.42 (2H, s), 5.94 (1H, d, J = 2.24 Hz), 5.83 (1H, d, J = 2.24 Hz), 5.35 (1H, m), 4.95 (1H, m), 3.87 (2H, t, J = 6.72 Hz), 2.93 (1H, dd, J = 17.14 and 4.50 Hz), 2.66 (1H, d, J = 17.12 Hz), 1.60 (6H, m), 1.27 (8H, m). ^{13}C NMR (100 MHz, DMSO-d$_6$): δ (ppm) = 165.03, 156.57, 156.49, 155.58, 150.75, 145.71, 138.91, 134.90, 133.54, 132.40, 130.19, 128.69, 124.11, 119.02, 118.17, 108.65, 105.47, 97.24, 95.54, 94.36, 71.73, 68.53, 67.44, 48.62, 38.10, 29.82, 29.36, 27.99, 25.12, 22.42, 13.92, 10.83.

2.5. Cell culture and treatments

The H9c2 cell line was bought from the National Centre for Cell Science (NCCS) Pune, India. They were grown in Dulbecco's Modified Eagle Medium (DMEM, provided with 10% fetal bovine serum (FBS), 1% pen-strep, and 0.2% amphotericin) at 37 °C in a humid environment with 5% CO_2. A mother stock with a concentration of 100 mM of EGCG and MitoEGCG$_n$ was prepared and stored at −20 °C until further usage. All treatments were done while maintaining the final DMSO concentration below 0.02%. DMSO treatment was considered as the control in every experiment. Cells were pretreated with different concentrations of EGCG, MitoEGCG$_n$ (where n = 4, 6, and 8) for 24 h and were thoroughly washed with 1X PBS twice post incubation. After washing, they were replenished with fresh medium containing 400 μM of H_2O_2 followed by incubation for another 20 min.

2.6. Measurement of *in vitro* radical scavenging activity

The total radical scavenging capacity of EGCG and MitoEGCG$_n$ compounds was measured using the DPPH assay protocol as reported earlier by our group.[16] Briefly, 0.2 mM stock solution of diphenyl picryl radical (DPPH) was prepared in 95% methanol at room temperature in dark. To obtain a final concentration of 0.1–200 μM for the EGCG or MitoEGCG$_n$ compounds (n = 4, 6, or 8), 150 μL of 0.2 mM DPPH solution was added to 50 μL, 4X DMSO stocks of the respective compounds. DMSO and ascorbic acid was taken as a negative and positive control respectively. The samples were incubated in a 96-well plate for 1 h at room temperature and in the dark. Using a microplate reader (BioTek, Epoch 2), the absorbance was measured at 517 nm after the allotted incubation time. The following formula was used to calculate the percentage of radical scavenging activity (RSA), where Abs$_s$ and Abs$_c$ stand for the sample's and the control's respective absorbances. Using GraphPad Prism software and non-linear regression analysis, IC$_{50}$ values were calculated.

$$\mathrm{RSA}(\%) = \left(\frac{\mathrm{Abs_c} - \mathrm{Abs_s}}{\mathrm{Abs_c}}\right) \times 100$$

2.7. Analysis of cell viability using MTT assay

The cell viability profile of rat cardiomyocyte cells, H9c2 after treatment with newly synthesized MitoEGCG$_n$ compounds, EGCG and in the experiments associated with H_2O_2 treatment were measured by using 3-(4,5-dimethylthiazol-2-yl)-2,5-diphenyltetrazolium bromide (MTT) assay. In short, 10 000 cells per well were seeded into the 96-well plates and treated according to the procedure mentioned in Section 2.5. Following the proper treatment and allotted incubation time, 10 μL of MTT solution (5 mg mL^{-1}) was added to each well and incubated for an additional 2 h. After carefully removing the medium, 100 μL DMSO was added to each well to dissolve the hydrophobic formazan crystals formed. Using a microplate

reader (BioTek, Epoch 2), the absorbance of the resultant blue solution was assessed at 590 nm and 620 nm (reference reading). IC_{50} values were determined using GraphPad Prism software and non-linear regression analysis.

2.8. Measurement of intracellular ROS using DCFH-DA staining

The intracellular ROS was accessed using 2′,7′-dichlorodihydrofluorescein diacetate (DCFH-DA) fluorescence assay. Briefly, H9c2 cells were seeded in 35 mm dishes at a density of 0.6×10^6 cells per dish and were allowed to adhere to the substratum overnight. Cells were incubated with EGCG and MitoEGCG$_n$ at 50 μM for 24 h in triplicates. After the stipulated time, one set of MitoEGCG$_n$ and EGCG treated cells was subjected to treatment with 400 μM H_2O_2 for 20 min and then incubated with 10 μM DCFH-DA reagent for 30 min. The media was removed after 30 min, cells were washed in 1X PBS and later supplemented with fresh media. The fluorescence was imaged using a fluorescence microscope (Olympus IX83) using ex/em wavelength of 485/530 nm.

2.9. Measurement of mitochondrial membrane potential

The change in mitochondrial membrane potential was measured fluorescently using TMRE reagent. Briefly, H9c2 cells were seeded in 35 mm dishes at a density of 0.3×10^6 cells per dish and were allowed to adhere to the substratum overnight. Cells were incubated with MitoEGCG$_n$ at various concentrations ranging from 0 to 100 μM for 24 h in duplicates. After the stipulated time, one set of MitoEGCG$_n$ treated cells was subjected to treatment with 400 μM H_2O_2 for 20 min and then incubated with TMRE 100 nM for 15 min. The media was removed after 30 min, cells were washed in 1X PBS and later supplemented with fresh media. The fluorescence images were acquired using a fluorescence microscope with ex/em wavelength of 544/570 nm.

2.10. Protein expression of pro-caspase 3 using western blotting

H9c2 cells were grown in 35 mm culture dishes and were subjected to pretreatment with 50 μM MitoEGCG$_4$, MitoEGCG$_6$ and EGCG for 24 h. After the pretreatment cells were washed twice with 1X PBS of pH 7.4 and replenished with fresh medium containing 400 μM H_2O_2 for 4 h. Following the treatment, cells were lysed in a lysis buffer containing 1% Triton X-100, 1% protease inhibitor cocktail, 100 mM DTT, 1 M Tris pH 7.4, 2 M NaCl, 0.1 M EDTA, and 10% glycerol. Bicinchoninic acid assay was used for estimating protein concentration. An equal amount of protein (40 μg) was separated on a 15% SDS-PAGE gel followed by transferring them to a PVDF membrane (Amersham) *via* western blotting. Afterwards, the membrane was blocked in 5% non-fat milk made with 1X PBST. The membrane was then incubated with the anti-pro-caspase 3 primary antibody at 4 °C overnight, after several washes in 1X PBST (3 times, 5 min each). It was again incubated further with HRP-conjugated anti-rabbit IgG secondary antibodies in 1X PBST for 2 h at room temperature, followed by the previously mentioned washing procedure. The same membrane was blotted against HRP conjugated anti β-actin antibody for loading control. Standard chemiluminescent substrate (ECL reagent, BioRad) was used for developing the membrane in both the cases. Densitometric intensities of bands of pro-caspase 3 were quantified using ImageJ software (NIH, USA) and normalized with respect to their corresponding loading controls (β-actin). The statistical analysis and graph were obtained using GraphPad Prism Software.

2.11. Statistical analysis

For the statistical analysis, GraphPad Prism 7 (GraphPad Software Inc., San Diego, CA, USA) was utilized. All the data are represented as mean ± standard error of the mean (SEM) from a minimum of three independent tests. A non-linear regression analysis was used to determine the IC_{50} values. One-way analysis of variance (ANOVA) with Dunnett's multiple comparison tests was used to analyze the statistical differences. The statistical significance was represented by the following symbols, 'ns' represents non-significance and is given for $p > 0.05$, * for $p < 0.05$, ** for $p < 0.01$, *** for $p < 0.001$, and **** for $p < 0.0001$.

3. Results and discussion

3.1. Synthesis and characterization of MitoEGCG$_n$

MitoEGCG$_n$ compounds were synthesized through a three-step process as shown in Scheme 1 starting from the dibromination of 1,*n*-alkanediols, where $n = 4$, 6, and 8. The resulting dibromoalkanes were reacted with EGCG to introduce the alkane linker to the 4″ position of EGCG *via* a nucleophilic substitution reaction in the presence of a weak base, NaOAc. The TPP was then introduced by the substitution of bromine in EGCG-C$_n$Br, where $n = 4$, 6, and 8. The MitoEGCG$_n$, ($n = 4$, 6, and 8) compounds were obtained with an overall 50–60% yield and >98.5% purity. They were characterized using LC-MS, HPLC and NMR (ESI Fig. S1–S12†).

The presence of multiple phenolic hydroxyl groups in EGCG makes it a good antioxidant substance by virtue of single-electron transfer mechanism. However, it is reported that EGCG tends to get destabilized and undergo rapid degradation and auto-oxidation in alkaline environments and physiological conditions.[15] Hence, several attempts have been made to stabilize the core pharmacophore of EGCG *via* small chemical modifications. Among the eight hydroxyl groups, one that is present in the 4″ position is the most acidic due to the presence of electron-withdrawing ester group at its *para* position and the characteristic resonance stabilization of the phenoxide ions. Previous studies from our group as well as other researchers have suggested that the substitution at 4″-OH does not alter the biological activities of EGCG. The introduction of alkyl groups of different chain lengths was found to increase the stability of EGCG.[16,17,23,24] The alkyl chain will also contribute to the increase in the lipophilicity of the compound and thus, the cellular uptake. Hence, we introduced the TPP moiety at the 4″ position of EGCG *via* an alkane chain linker anticipating its favorable cellular uptake and mitochondrial targeting. Of note,

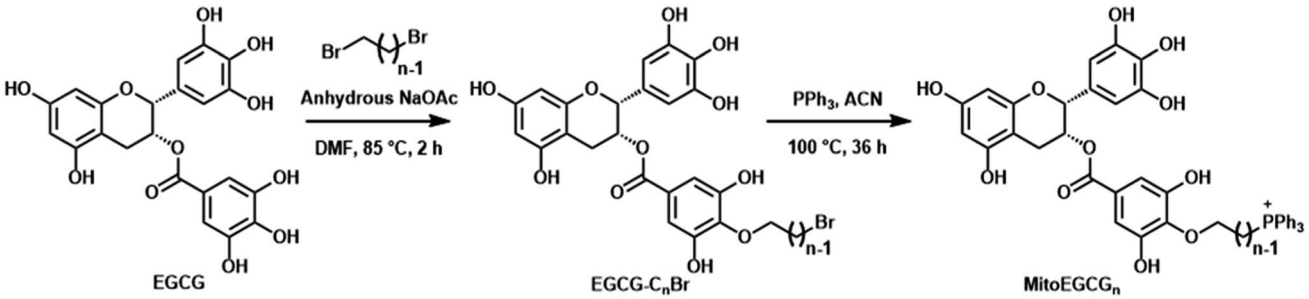

Scheme 1 Synthetic route for MitoEGCG$_n$ where n = 4, 6, and 8.

TPP is a well-established moiety to target compounds into the mitochondria.

3.2. Antioxidant property of MitoEGCG$_n$ compounds

EGCG is widely known as an antioxidant agent as it can effectively scavenge the ROS. In order to evaluate whether the structural modification performed at 4″ position of EGCG to introduce TPP has any influence on the native antioxidant activity of EGCG, we performed a radical scavenging activity analysis using *in vitro* DPPH assay. In DPPH assay, the antioxidant activity of EGCG and MitoEGCG$_n$ compounds were measured as the capacity to reduce the stable DPPH radical (violet) into a colorless reduced DPPH molecule. Here, ascorbic acid was taken as the positive control or reference compound which is known to be an effective antioxidant compound. The antioxidant properties of MitoEGCG$_n$ (IC_{50} of MitoEGCG$_4$ = 11.04 ± 0.02 μM, MitoEGCG$_6$ = 13.32 ± 0.02 μM and MitoEGCG$_8$ = 12.98 ± 0.04 μM) were not compromised upon the addition of TPP linked alkyl chains to EGCG (IC_{50} of EGCG being 7.69 ± 0.02 μM) (Fig. 1a and b). In fact, they remain better antioxidant agents than well-known antioxidant, ascorbic acid (IC_{50} = 28.67 ± 0.01 μM). Mitochondria are considered as the primary source of ROS generation mainly due to the transport of electrons through the various complexes of electron transport chain for the sake of ATP production in the cells.[25,26] Thus, targeting EGCG directly to mitochondria using TPP ion conjugation is expected to exert potent reduction in the damage induced by the ROS.

3.3. MitoEGCG$_n$ derivatives do not show toxicity to H9c2 cells

Progression of cardiovascular disease-related conditions are commonly associated with the accumulation of oxidative stress.[27,28] The H9c2 cell lines are widely used for studying cardiac function and disease conditions because they have many characteristics similar to cardiac myocytes, the cells responsible for contraction in the heart. We used rat cardiomyocytes (H9c2 cell line) treated with H_2O_2 to create a cellular model for cardiac tissues in response to oxidative stress conditions.[22,29] In order to select the effective concentration of H_2O_2 in inducing cellular damage to H9c2 cells, cell viability was assessed in the presence of different concentrations of H_2O_2 (0–1000 μM) with different duration of treatments (Fig. 2a). Treatment with 400 μM H_2O_2 for 20 min induced 30.81% loss in cell viability of H9c2 cells which further increased with increase in time of incubation. The effect of MitoEGCG$_n$ compounds on the cell viability of H9c2 cells was also analyzed using the MTT assay and was compared with that of the parent compound, EGCG. We observed that, where EGCG was non-toxic to cells only up to 50 μM (Fig. 2b), MitoEGCG$_4$

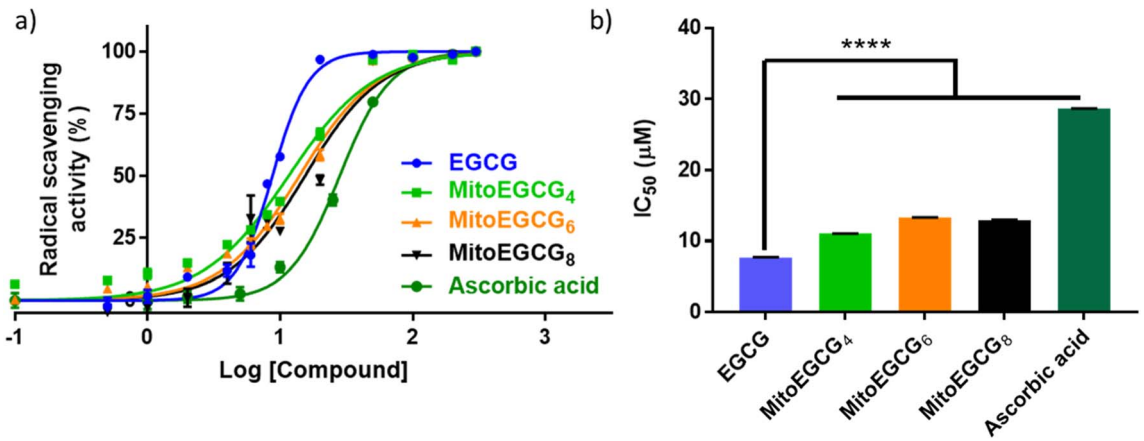

Fig. 1 (a) *In vitro* antioxidant profiles of EGCG, MitoEGCG$_4$, MitoEGCG$_6$, MitoEGCG$_8$ and ascorbic acid as derived from DPPH assay, (b) comparison and evaluation of IC_{50} values of EGCG, MitoEGCG$_4$, MitoEGCG$_6$, MitoEGCG$_8$ and ascorbic acid obtained from DPPH assay. Data are expressed as mean ± standard error of the mean (SEM) and **** represents $p < 0.0001$.

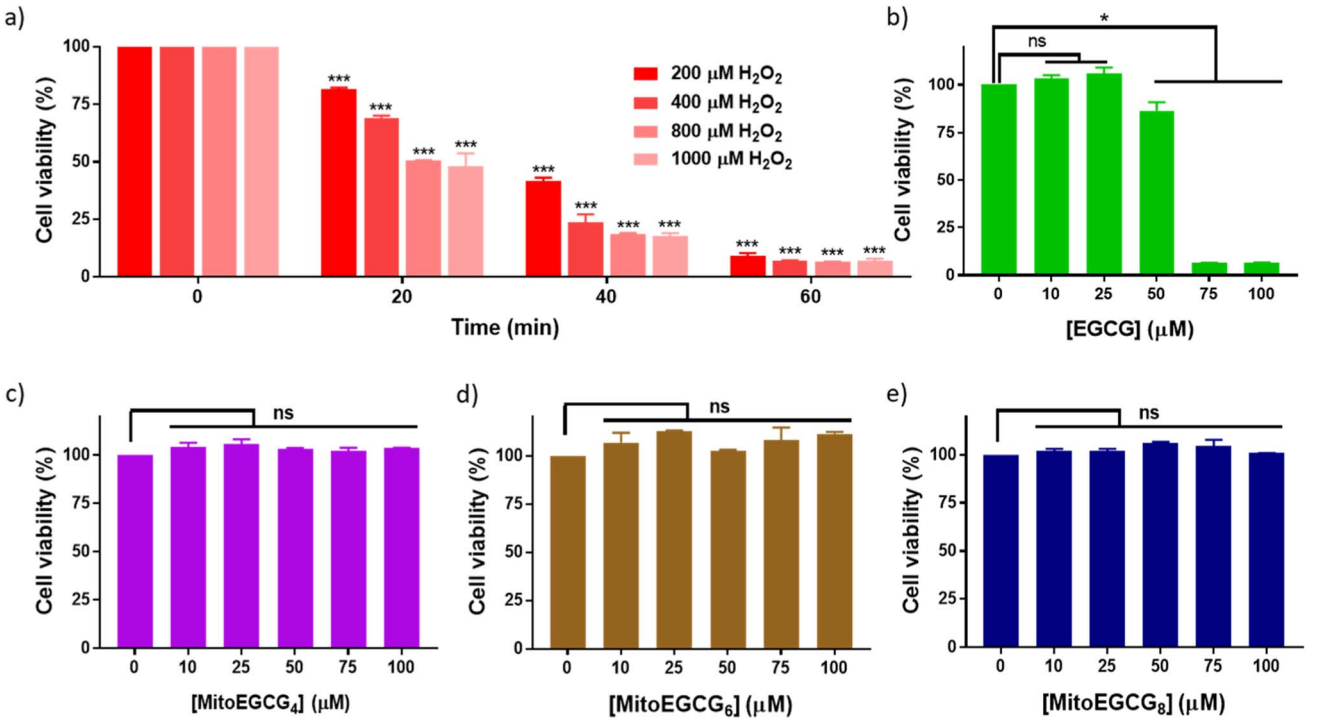

Fig. 2 Cell viability of H9c2 cells treated with (a) different concentrations of H_2O_2 (0–1000 μM) at different time points (0–60 min), (b) EGCG for 24 h, (c) MitoEGCG$_4$ for 24 h, (d) MitoEGCG$_6$ for 24 h and (e) MitoEGCG$_8$ for 24 h. All the experiments have been conducted in triplicates. ***p < 0.001 compared with respective treatment for 0 min, ns denotes p > 0.05 (non-significance) and *p < 0.05 as compared to DMSO control.

(Fig. 2c), MitoEGCG$_6$ (Fig. 2d), and MitoEGCG$_8$ (Fig. 2e) were not toxic to cells even at higher concentrations of 100 μM. This observation suggested that MitoEGCG$_n$ compounds could predominantly behave like an antioxidant at higher concentrations where the parent molecule (EGCG) exerts pro-oxidant activity thus, killing the cells. Hence, it was imperative to analyze the action of MitoEGCG$_n$ compounds in the presence of H_2O_2 treatment, a potential stress condition leading to further cellular damage.

3.4. MitoEGCG$_n$ alleviated the damage induced by H_2O_2 on H9c2 cells

In order to evaluate the protective effect of MitoEGCG$_n$ compounds against H_2O_2-induced oxidative stress, we pre-treated H9c2 cells with different concentrations of EGCG, MitoEGCG$_4$, MitoEGCG$_6$ and MitoEGCG$_8$ separately for 24 h and later subjected to oxidative stress by treating them further with 400 μM H_2O_2 for 20 min. The cell viability analysis demonstrated that MitoEGCG$_4$, and MitoEGCG$_6$ both protected the H9c2 cell lines from the oxidative damage induced by H_2O_2 from the concentration of 50 μM whereas EGCG failed to exhibit its antioxidant activity (Fig. 3a and b). MitoEGCG$_8$ was however unable to show similar results as exhibited by its lower alkyl chain counterparts (Fig. 3a–c) This observation could be attributed to the increased hydrophobicity of MitoEGCG$_8$ which restricts its entry inside the mitochondrial matrix.[30] The inverted bright field image of cells in Fig. 3d and ESI Fig. S10 and S11† clearly show that both MitoEGCG$_4$ and MitoEGCG$_6$ protected H9c2 cells from the damage induced by H_2O_2 in comparison to EGCG. Importantly, EGCG alone was found to be toxic. Our findings substantiate the potential of mitochondrial targeting of EGCG to protect cells from severe oxidative stress. The antioxidative property of EGCG is widely utilized therapy for healing and cell survival in case of several life-threatening pathological diseases including cardiovascular diseases.[31,32] However, depending on the concentration used and the prevalent redox environment, EGCG is known to exert prooxidant activity in addition to its antioxidant action.[33] Interestingly, MitoEGCG$_4$ and MitoEGCG$_6$ were able to exhibit their antioxidant activity even at higher doses where EGCG mostly start behaving as a prooxidant. These observations strongly suggest that MitoEGCG$_4$ and MitoEGCG$_6$ targeted EGCG into the mitochondria and were involved in quenching the ROS produced inside the mitochondria. Further experiments to understand the mechanistic underlying were performed with MitoEGCG$_4$ and MitoEGCG$_6$.

3.5. MitoEGCG$_n$ scavenged the ROS generated by the action of H_2O_2 treatment

H_2O_2 treatment to cells is a widely used procedure to induce ROS generation which ultimately promotes cellular injury. In order to determine the mechanism of action behind the activity of MitoEGCG$_n$ compounds in effectively reducing H_2O_2-induced cell death, intracellular ROS generation was determined using 2′,7′-dichlorodihydro fluorescein diacetate (DCFH-DA) staining analysis. DCFH-DA is a cell-permeable non-fluorescent dye which in the presence of esterases inside the cell gets hydrolyzed upon cellular absorption to produce 2′,7′-

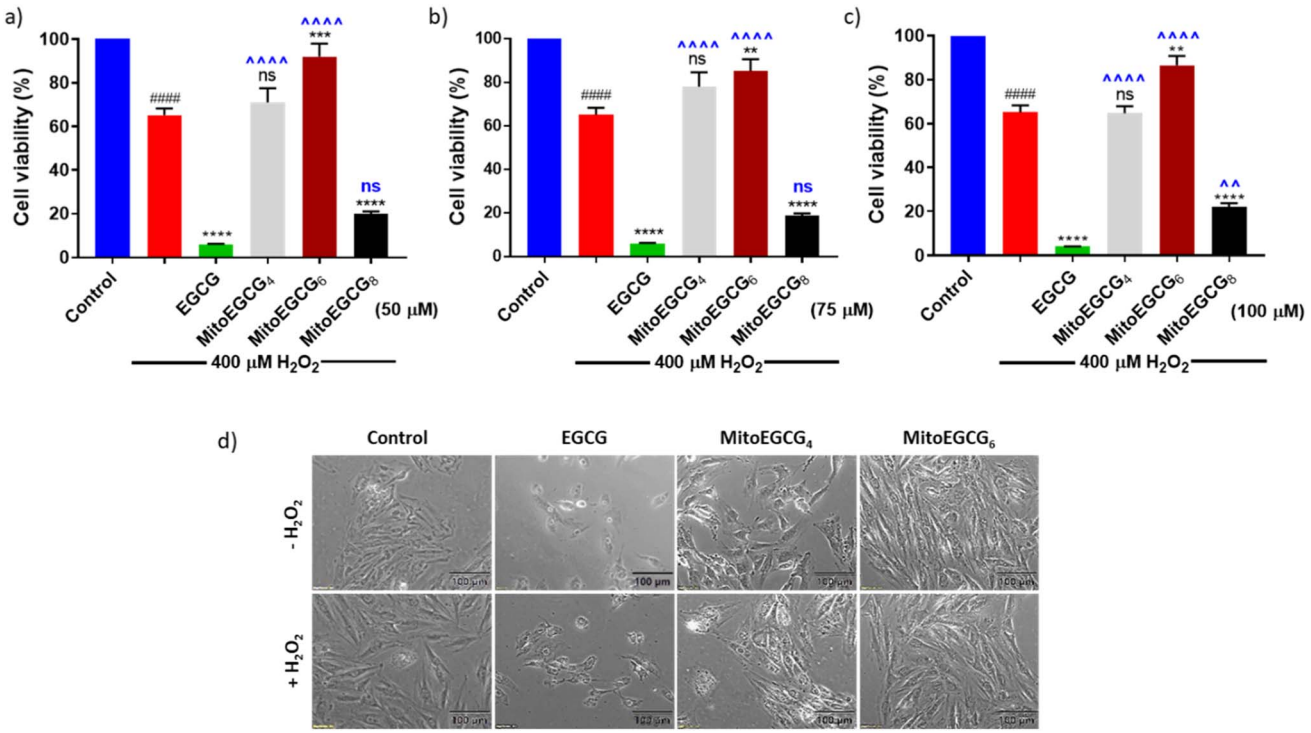

Fig. 3 Bar diagram showing cell viability of H9c2 cells treated with (a) 50 μM, (b) 75 μM, (c) 100 μM of EGCG, MitoEGCG$_4$, MitoEGCG$_6$ and MitoEGCG$_8$ in the presence of 400 μM H_2O_2 for 20 min. All experiments were conducted in triplicates and statistical significance was denoted as follows: ####p < 0.0001 as compared to control. ns represents non-significance and **p < 0.01, ***p < 0.001 and ****p < 0.0001 as compared to H_2O_2 treated samples. ns represents non-significance ^^p < 0.01, and ^^^^p < 0.0001 as compared to EGCG treated samples (one-way ANOVA with Dunnett's multiple-comparison post-test) and (d) Inverted microscopic images of H9c2 cells pretreated with 50 μM of EGCG, MitoEGCG$_4$, and MitoEGCG$_6$ and then kept in media with and without H_2O_2 (200 μM). Magnification 20×. Cell viability was assessed using an MTT assay.

dichlorodihydrofluorescein (DCFH), which is then oxidized by ROS to produce a green fluorescent 2′,7′-dichlorofluorescein (DCF) molecule. As the intracellular ROS generation is directly proportional to the intensity of the fluorescence, this reagent can be used to determine the amount of ROS produced inside the cell in the presence of different antioxidants. From the DCFH-DA staining results it is evident that MitoEGCG$_4$ and MitoEGCG$_6$ effectively protected the H9c2 cells by scavenging the ROS resulted from H_2O_2 treatment. It was also noticed that EGCG was unable to impart any significant antioxidant effect on H_2O_2 treatment (Fig. 4a and b and ESI Fig. S13†). This further provides the evidence that the TPP-linked mitochondrial-targeting EGCG derivatives protect cells from the ROS-induced cell damage by scavenging them.

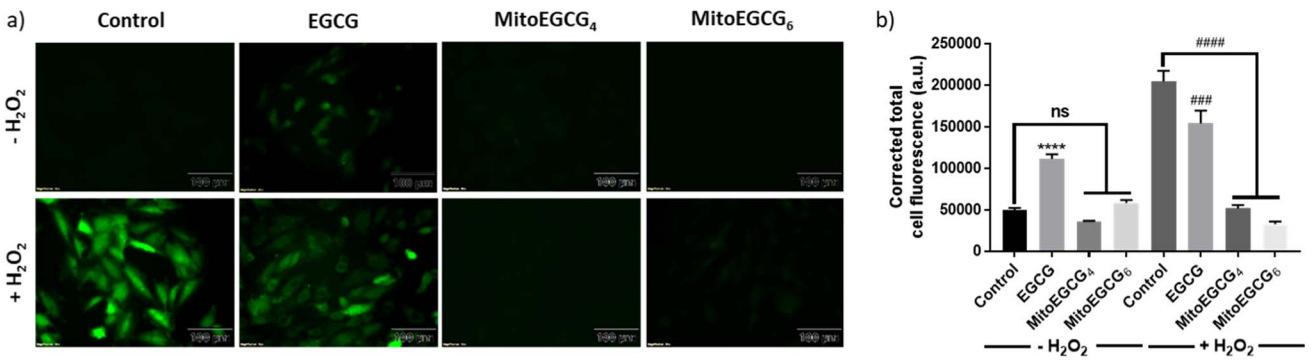

Fig. 4 (a) Fluorescence microscopic images of DCFH-DA stained H9c2 cells pretreated with DMSO (control), 50 μM of EGCG, MitoEGCG$_4$, and MitoEGCG$_6$ and then kept in media with and without H_2O_2 (50 μM). Images were acquired at an ex/em wavelength of 485/530 nm and (b) Corresponding relative fluorescence intensity calculated using ImageJ software and statistical analysis was done using GraphPad Prism software. Data are represented as a mean ± SEM, $n = 10$. ns represents non significance and ****p < 0.0001 as compared to control (−H_2O_2). ###p < 0.001, and ####p < 0.0001 as compared to control (+H_2O_2) (one-way ANOVA with Dunnett's multiple-comparison post-test).

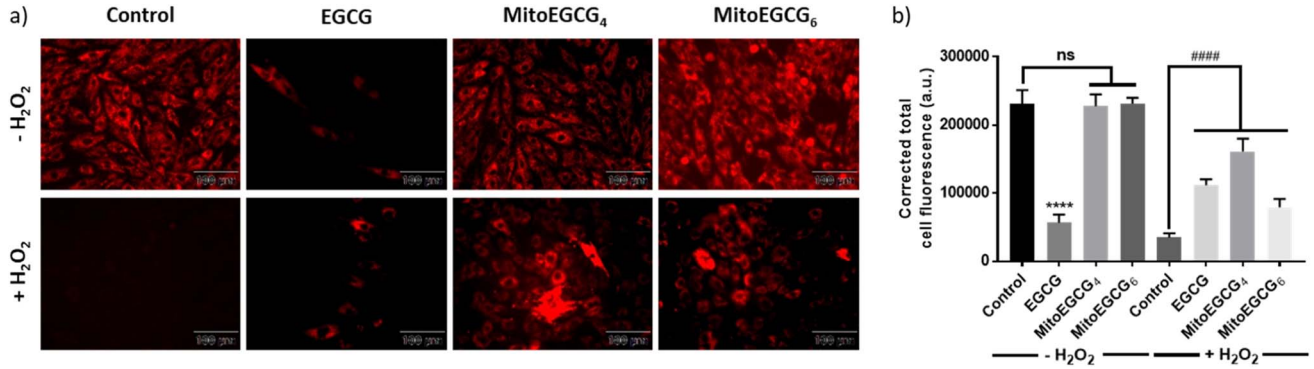

Fig. 5 (a) Fluorescence microscopic images of TMRE stained H9c2 cells pretreated with DMSO (control), 50 μM of EGCG, MitoEGCG$_4$, and MitoEGCG$_6$ and then kept in media with and without H_2O_2 (400 μM). Images were acquired at an ex/em range of 552/574 nm and (b) Corresponding relative fluorescence intensity was calculated using ImageJ software and statistical analysis was done using GraphPad Prism software. Data are represented as a mean ± SEM, $n = 10$. ns represents non significance and ****$p < 0.0001$ as compared to control ($-H_2O_2$). Wereas ####$p < 0.0001$ as compared to control ($+H_2O_2$) (one-way ANOVA with Dunnett's multiple-comparison post-test).

3.6. MitoEGCG$_n$ protected H9c2 cells from H_2O_2-induced damage by preventing the loss of mitochondrial outer membrane potential (Ψ_m)

To examine the effect of MitoEGCG$_4$ and MitoEGCG$_6$ on the H_2O_2-induced mitochondrial potential disruption, we measured the mitochondrial potential of MitoEGCG$_4$ and MitoEGCG$_6$ treated cells in the presence and absence of H_2O_2 by staining the cells with tetramethylrhodamine ethyl ester (TMRE). TMRE is a cell-permeant cationic dye that can accumulate inside the mitochondria due to the higher negative potential of the

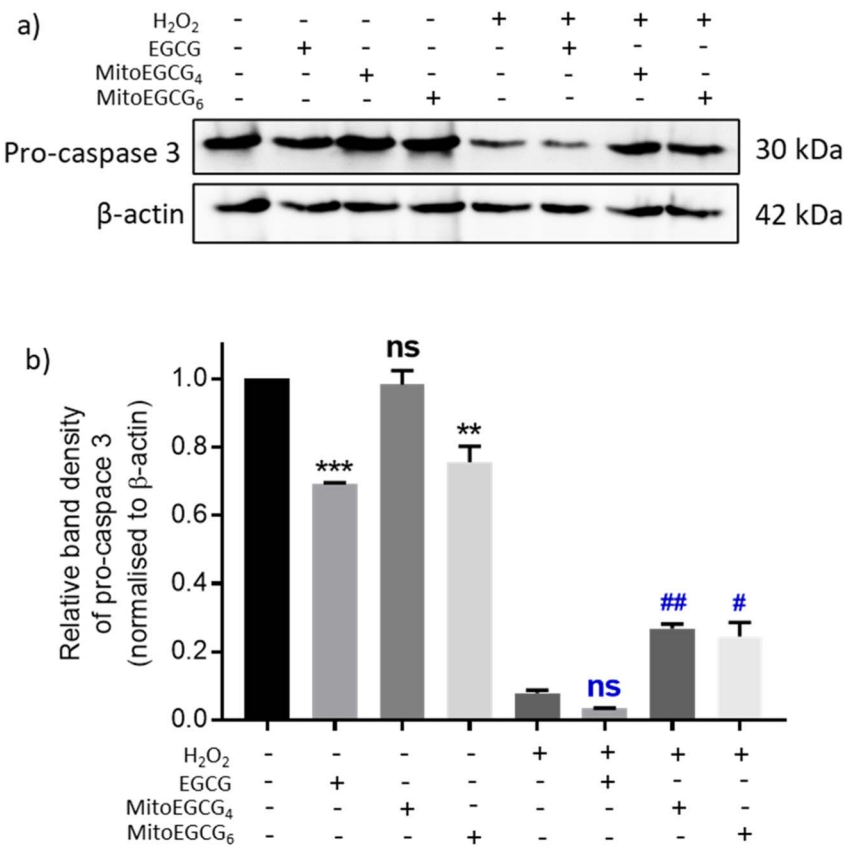

Fig. 6 MitoEGCG$_4$ protected H9c2 cell lines from H_2O_2-induced activation of pro-caspase 3. (a) Western blot analysis depicting pro-caspase 3 protein expression in cells pretreated with EGCG, MitoEGCG$_4$ and MitoEGCG$_6$ and further exposed to 400 μM of H_2O_2 for 4 h and (b) density gradient graph prepared by measuring the band density of pro-caspase 3 in each lane and normalizing against the loading control. All the data were represented as mean ± standard error of the mean (SEM) from at least 3 independent experiments. ns represents non significance, **$p <$ 0.01 and ***$p < 0.001$ as compared to control ($-H_2O_2$). Whereas ns represents non significance ($p > 0.05$) and ##$p < 0.01$ as compared to control ($+H_2O_2$) (one-way ANOVA with Dunnett's multiple-comparison post-test).

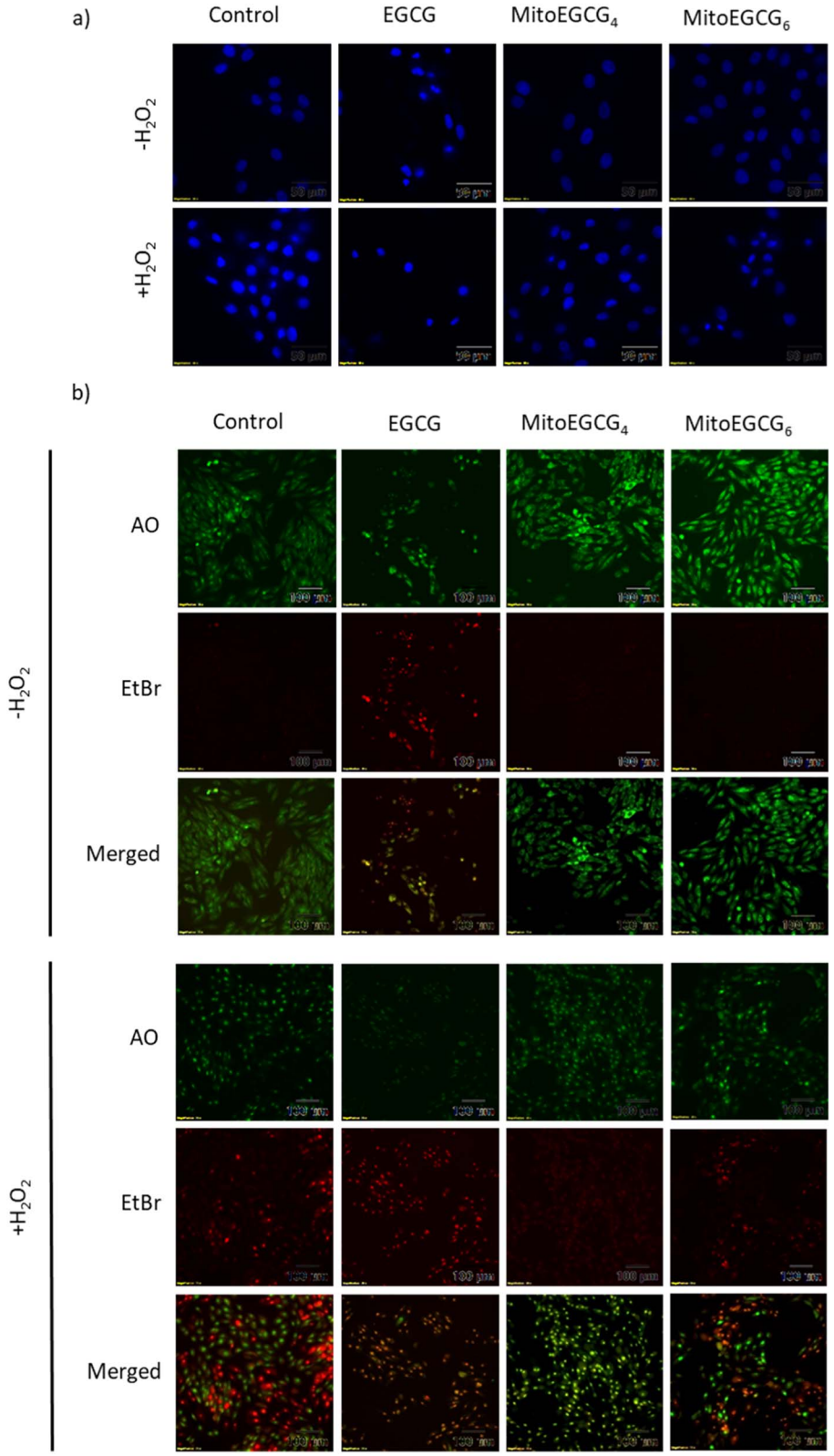

Fig. 7 MitoEGCG$_4$ protected H9c2 cell lines from H_2O_2-induced activation of apoptosis (a) Hoechst staining of cells pretreated with EGCG, MitoEGCG$_4$ and MitoEGCG$_6$ in the absence and presence of H_2O_2 (400 μM) and (b) AO/EtBr staining of cells pretreated with EGCG, MitoEGCG$_4$ and MitoEGCG$_6$ in the presence and absence of H_2O_2 (400 μM).

mitochondria.[34] Mitochondrial function is highly regulated by the mitochondrial outer membrane potential (Ψ_m) and it plays an important role in mitochondrial biogenesis and metabolism.[35–37] Pretreatment of MitoEGCG$_4$ and MitoEGCG$_6$ attenuated the loss of Ψ_m induced by H_2O_2 treatment in H9c2 cells in comparison to EGCG. It was also observed that EGCG was reducing the Ψ_m of cells at concentrations above 50 μM and therefore acting as a pro-oxidant to cardiomyocyte cells (Fig. 5a and b and ESI Fig. S14†). The disruption of Ψ_m in cardiomyocyte cells is ascribed to the initiation of oxidative stress in the physiology of cardiomyopathies.[20,38–40] EGCG has been extensively demonstrated for regulating mitochondrial health, biogenesis, ATP production, mitochondrial metabolism, and bioenergetics. Furthermore, EGCG has also been known to regulate mitochondrial redox levels by modulating antioxidant enzymes, and Ca^{2+} influx system in the cell *etc.*[41–43] Hence, targeting EGCG directly inside the mitochondria which is the central hub for ROS species generation results in loss in Ψ_m may prove effective in protecting the cells from oxidative stress. As expected, our results targeted EGCG into the mitochondrial matrix and protected the mitochondrial functions and thereby, helped the fight against the injury induced through H_2O_2 treatment.

3.7. MitoEGCG$_n$ ameliorated H_2O_2-induced apoptosis in H9c2 cell line

Disruption in mitochondrial outer membrane potential is associated with the activation of intrinsic apoptosis pathway. H_2O_2 treatment in many cases has been well documented in inducing mitochondria-dependent apoptosis pathway which involves a loss in mitochondrial membrane potential followed by release of cytochrome c, which ultimately results in the activation of caspase.[44] In order to assess the capability of MitoEGCG$_4$ and MitoEGCG$_6$ in protecting the cells from H_2O_2-induced apoptosis activation, we performed the western blot analysis to assess the pro-caspase 3 level. The data clearly show that MitoEGCG$_4$ and MitoEGCG$_6$ effectively protected the cells from H_2O_2-induced caspase 3 activation in comparison to EGCG (Fig. 6a and b and ESI Fig. S15†). It was observed that EGCG in the tested concentration exhibited pro-oxidant activity in H9c2 cells and as a result, EGCG-treated cells completely succumbed to cell death in the presence of H_2O_2 treatment (Fig. 3d and ESI Fig. S13 and S14†). Activation of caspase 3 in cells further leads to downstream cleavage of oligonucleosomal DNA which can easily be detected using Hoechst staining of cells. As shown in Fig. 7a, MitoEGCG$_4$ and MitoEGCG$_6$-pretreated cells retained the status of healthy nucleus in the presence of H_2O_2 treatment. This result indicated the antioxidant ability of MitoEGCG$_4$ and MitoEGCG$_6$ in protecting the cells from H_2O_2-induced cell injury. We also examined the integrity of cell membrane of H9c2 cells with similar treatment. It was observed that H_2O_2 was unable to induce loss in membrane integrity in the cells pretreated with MitoEGCG$_4$ and MitoEGCG$_6$ to the same extent (Fig. 7b). The aforementioned results demonstrated that sequestering EGCG into the mitochondria by pretreating cells with MitoEGCG$_n$ protected them from H_2O_2-induced cell death.

4. Conclusion

A series of mitochondrial-targeting EGCG probes, namely MitoEGCG$_n$, were synthesized *via* conjugating a triphenylphosphonium ion with EGCG at its 4″ position using alkyl chain linkers of different hydrophobicity. MitoEGCG$_4$ and MitoEGCG$_6$ were found to be effective in protecting the cells from H_2O_2-induced cell injury as revealed by the MTT analysis, unlike EGCG that was unable to exhibit any such cytoprotection. On further probing the mechanism of the protective effect rendered by MitoEGCG$_4$ and MitoEGCG$_6$ against H_2O_2 treatment in rat cardiomyocyte cells, we observed that these compounds imparted an antioxidant effect to the cells by reducing the production of ROS produced by H_2O_2 treatment in cells. We also demonstrated that MitoEGCG$_4$ and MitoEGCG$_6$ protected the mitochondria of the cells from H_2O_2-induced loss in the outer mitochondrial membrane potential, thereby also blocking the activation of intrinsic apoptotic pathway. Cells pretreated with MitoEGCG$_4$ and MitoEGCG$_6$ did not show caspase activation as well as other apoptotic features like nuclear fragmentation and loss in membrane integrity. Thereby, our findings unequivocally demonstrate that MitoEGCG$_4$ and MitoEGCG$_6$ both functioned as antioxidants within the mitochondria, preventing H_2O_2-induced cell damage. However, further investigation is warranted to fully comprehend the mechanisms behind the protective benefits of MitoEGCG$_n$ compounds against H_2O_2-induced cardiomyocyte mitochondrial damage.

Conflicts of interest

The authors declare no conflict of interest.

Acknowledgements

We sincerely acknowledge the Indian Institute of Technology (IIT) Palakkad, India for the facilities and support provided to carry out this work. We also acknowledge the funding from the Council of Scientific & Industrial Research (CSIR), India (02(0434)/21/EMR-II and 09/1282(0003)/2019-EMR-I) and the National Post-doctoral Fellowship (NPDF), Science and Engineering Research Board (SERB), India (PDF/2020/001950). We greatly acknowledge the Central Instrumentation Facility (CIF) of IIT Palakkad for the technical support and the Central Instrumentation Centre (CIC), Bharathiar University supported by DST (PURSE Phase II program), New Delhi for the NMR analysis.

References

1 G. Siasos, V. Tsigkou, M. Kosmopoulos, D. Theodosiadis, S. Simantiris, N. M. Tagkou, A. Tsimpiktsioglou, P. K. Stampouloglou, E. Oikonomou, K. Mourouzis, A. Philippou, M. Vavuranakis, C. Stefanadis, D. Tousoulis and A. G. Papavassiliou, Mitochondria and cardiovascular diseases from pathophyiology to treatment, *Ann. Transl. Med.*, 2018, **6**, 256.

2 K. Chaudhari, B. Hamad and B. A. Syed, Antithrombotic drugs market, *Nat. Rev. Drug Discovery*, 2014, **13**, 571–572.
3 C. L. Li, M. H. Dong, Y. J. Ren and L. H. Li, Design, synthesis, biological evaluation and molecular docking of novel dabigatran derivatives as potential thrombin inhibitors, *RSC Adv.*, 2015, **5**, 23737–23748.
4 X. Zhu and L. Zuo, Characterization of oxygen radical formation mechanism at early cardiac ischemia, *Cell Death Dis.*, 2013, **4**, e787.
5 C. Y. Mao, H. Bin Lu, N. Kong, J. Y. Li, M. Liu, C. Y. Yang and P. Yang, Levocarnitine protects H9c2 rat cardiomyocytes from H2O2-induced mitochondrial dysfunction and apoptosis, *Int. J. Med. Sci.*, 2014, **11**, 1107–1115.
6 M. Chiong, Z. V. Wang, Z. Pedrozo, D. J. Cao, R. Troncoso, M. Ibacache, A. Criollo, A. Nemchenko, J. A. Hill and S. Lavandero, Cardiomyocyte death: Mechanisms and translational implications, *Cell Death Dis.*, 2011, **2**, e244.
7 K. Konstantinidis, R. S. Whelan and R. N. Kitsis, Mechanisms of cell death in heart disease, *Arterioscler., Thromb., Vasc. Biol.*, 2012, **32**, 1552–1562.
8 G. S. Gorman, P. F. Chinnery, S. DiMauro, M. Hirano, Y. Koga, R. McFarland, A. Suomalainen, D. R. Thorburn, M. Zeviani and D. M. Turnbull, Mitochondrial diseases, *Nat. Rev. Dis. Prim.*, 2016, **2**, 16080.
9 P. Martín-Maestro, R. Gargini, E. García, G. Perry, J. Avila and V. García-Escudero, Slower dynamics and aged mitochondria in Sporadic Alzheimer's disease, *Oxid. Med. Cell. Longevity*, 2017, **2017**, 9302761.
10 L. Basiricò, P. Morera, D. Dipasquale, R. Bernini, L. Santi, A. Romani, N. Lacetera and U. Bernabucci, (−)-Epigallocatechin-3-gallate and hydroxytyrosol improved antioxidative and anti-inflammatory responses in bovine mammary epithelial cells, *Animal*, 2019, **13**, 2847–2856.
11 S. Bettuzzi, M. Brausi, F. Rizzi, G. Castagnetti, G. Peracchia and A. Corti, Chemoprevention of human prostate cancer by oral administration of green tea catechins in volunteers with high-grade prostate intraepithelial neoplasia: A preliminary report from a one-year proof-of-principle study, *Cancer Res.*, 2006, **66**, 1234–1240.
12 Y. Du, H. Ding, K. Vanarsa, S. Soomro, S. Baig, J. Hicks and C. Mohan, Low dose epigallocatechin gallate alleviates experimental colitis by subduing inflammatory cells and cytokines, and improving intestinal permeability, *Nutrients*, 2019, **11**, 1743.
13 Q. Y. Eng, P. V. Thanikachalam and S. Ramamurthy, Molecular understanding of Epigallocatechin gallate (EGCG) in cardiovascular and metabolic diseases, *J. Ethnopharmacol.*, 2018, **210**, 296–310.
14 A. Binoy, D. Nedungadi, N. Katiyar, C. Bose, S. A. Shankarappa, B. G. Nair and N. Mishra, Plumbagin induces paraptosis in cancer cells by disrupting the sulfhydryl homeostasis and proteasomal function, *Chem.-Biol. Interact.*, 2019, **310**, 108733.
15 R. Sahadevan, S. Singh, A. Binoy and S. Sadhukhan, Chemico-biological aspects of (−)-epigallocatechin-3-gallate (EGCG) to improve its stability, bioavailability and membrane permeability: Current status and future prospects, *Crit. Rev. Food Sci. Nutr.*, 2022, 1–30.
16 R. Sahadevan, A. Binoy, S. K. Vechalapu, P. Nanjan and S. Sadhukhan, In situ global proteomics profiling of EGCG targets using a cell-permeable and Click-able bioorthogonal probe, *Int. J. Biol. Macromol.*, 2023, **237**, 123991.
17 S. Singh, R. Sahadevan, R. Roy, M. Biswas, P. Ghosh, P. Kar, A. Sonawane and S. Sadhukhan, Structure-based design and synthesis of a novel long-chain 4″-alkyl ether derivative of EGCG as potent EGFR inhibitor: in vitro and in silico studies, *RSC Adv.*, 2022, **12**, 17821–17836.
18 C. Minnelli, L. Cianfruglia, E. Laudadio, M. Giovanna, R. Galeazzi and T. Armeni, Effect of epigallocatechin-3-gallate on egfr signaling and migration in non-small cell lung cancer, *Int. J. Mol. Sci.*, 2021, **22**, 11833.
19 J. Zielonka, J. Joseph, A. Sikora, M. Hardy, O. Ouari, J. Vasquez-Vivar, G. Cheng, M. Lopez and B. Kalyanaraman, Mitochondria-targeted triphenylphosphonium-based compounds: Syntheses, mechanisms of action, and therapeutic and diagnostic applications, *Chem. Rev.*, 2017, **117**, 10043–10120.
20 J. S. Bhatti, G. K. Bhatti, P. H. Reddy, U. States, U. States, U. States, H. S. Departments, U. States, S. W. Campus and U. States, Mitochondrial dysfunction and oxidative stress in metabolic disorders - A step towards mitochondria based therapeutic strategies, *Biochim. Biophys. Acta*, 2018, **1863**, 1066–1077.
21 L. Zhang, Y. Liu, J. Y. Li, L. Z. Li, Y. L. Zhang, H. Y. Gong and Y. Cui, Protective effect of rosamultin against H2O2 -induced oxidative stress and apoptosis in H9c2 cardiomyocytes, *Oxid. Med. Cell. Longevity*, 2018, 8415610.
22 E. Son, D. Lee, C. W. Woo and Y. H. Kim, The optimal model of reperfusion injury in vitro using H9c2 transformed cardiac myoblasts, *Korean J. Physiol. Pharmacol.*, 2020, **24**, 173–183.
23 M. Maeda-Yamamoto, N. Inagaki, J. Kitaura, T. Chikumoto, H. Kawahara, Y. Kawakami, M. Sano, T. Miyase, H. Tachibana, H. Nagai and T. Kawakami, O-methylated catechins from tea leaves inhibit multiple protein kinases in mast cells, *J. Immunol.*, 2004, **172**, 4486–4492.
24 M. Suzuki, K. Yoshino, M. Maeda-Yamamoto, T. Miyase and M. Sano, Inhibitory effects of tea catechins and O-methylated derivatives of (−)-epigallocatechin-3-O-gallate on mouse type IV allergy, *J. Agric. Food Chem.*, 2000, **48**, 5649–5653.
25 M. P. Murphy, How mitochondria produce reactive oxygen species, *Biochem. J.*, 2009, **417**, 1–13.
26 Q. Chen, E. J. Vazquez, S. Moghaddas, C. L. Hoppel and E. J. Lesnefsky, Production of reactive oxygen species by mitochondria: Central role of complex III, *J. Biol. Chem.*, 2003, **278**, 36027–36031.
27 Y. Kayama, U. Raaz, A. Jagger, M. Adam, I. N. Schellinger, M. Sakamoto, H. Suzuki, K. Toyama, J. M. Spin and P. S. Tsao, Diabetic cardiovascular disease induced by oxidative stress, *Int. J. Mol. Sci.*, 2015, **16**, 25234–25263.

28 G. Pizzino, N. Irrera, M. Cucinotta, G. Pallio, F. Mannino, V. Arcoraci, F. Squadrito, D. Altavilla and A. Bitto, Oxidative stress: Harms and benefits for human health, *Oxid. Med. Cell. Longevity*, 2017, 8416763.

29 H. C. Chou, Y. W. Chen, T. R. Lee, F. S. Wu, H. T. Chan, P. C. Lyu, J. F. Timms and H. L. Chan, Proteomics study of oxidative stress and Src kinase inhibition in H9C2 cardiomyocytes: a cell model of heart ischemia-reperfusion injury and treatment, *Free Radicals Biol. Med.*, 2010, **49**, 96–108.

30 M. F. Ross, T. A. Prime, I. Abakumova, A. M. James, C. M. Porteous, R. A. J. Smith and M. P. Murphy, Rapid and extensive uptake and activation of hydrophobic triphenylphosphonium cations within cells, *Biochem. J.*, 2008, **411**, 633–645.

31 W. Zhang, L. Chen, Y. Xiong, A. C. Panayi, A. Abududilibaier, Y. Hu, C. Yu, W. Zhou, Y. Sun, M. Liu, H. Xue, L. Hu, C. Yan, X. Xie, Z. Lin, F. Cao, B. Mi and G. Liu, Antioxidant therapy and antioxidant-related bionanomaterials in diabetic wound healing, *Front. Bioeng. Biotechnol.*, 2021, **9**, 707479.

32 S. Shaban, M. W. A. El-Husseny, A. I. Abushouk, A. M. A. Salem, M. Mamdouh and M. M. Abdel-Daim, Effects of antioxidant supplements on the survival and differentiation of stem cells, *Oxid. Med. Cell. Longevity*, 2017, **2017**, 5032102.

33 H. S. Kim, M. J. Quon and J. Kim, New insights into the mechanisms of polyphenols beyond antioxidant properties; lessons from the green tea polyphenol, epigallocatechin 3-gallate, *Redox Biol.*, 2014, **2**, 187–195.

34 L. C. Crowley, M. E. Christensen and N. J. Waterhouse, Measuring mitochondrial transmembrane potential by TMRE staining, *Cold Spring Harb. Protoc.*, 2016, **2016**, 1092–1096.

35 M. R. De Oliveira, S. F. Nabavi, M. Daglia, L. Rastrelli and S. M. Nabavi, Epigallocatechin gallate and mitochondria - A story of life and death, *Pharmacol. Res.*, 2016, **104**, 70–85.

36 J. Ren, P. Lakshmi, A. Whaley-Connell and J. R. Sowers, Mitochondrial biogenesis in the metabolic syndrome and cardiovascular disease, *J. Mol. Med.*, 2010, **88**, 993–1001.

37 A. Braczko, B. Kutryb-Zajac, A. Jedrzejewska, O. Krol, P. Mierzejewska, M. Zabielska-Kaczorowska, E. M. Slominska and R. T. Smolenski, Cardiac mitochondria dysfunction in dyslipidemic mice, *Int. J. Mol. Sci.*, 2022, **23**, 11488.

38 C. Y. Guo, L. Sun, X. P. Chen and D. S. Zhang, Oxidative stress, mitochondrial damage and neurodegenerative diseases, *Neural Regener. Res.*, 2013, **8**, 2003–2014.

39 E. Marzetti, A. Csiszar, D. Dutta, G. Balagopal, R. Calvani and C. Leeuwenburgh, Role of mitochondrial dysfunction and altered autophagy in cardiovascular aging and disease: From mechanisms to therapeutics, *Am. J. Physiol. Heart Circ. Physiol.*, 2013, **305**, H459–H476.

40 T. Autumn, E. K. Quarles, N. Basisty, L. Gitari and P. S. Rabinovitch, Mitochondrial dysfunction in cardiac ageing, *Biochim. Biophys. Acta*, 2015, **1847**, 1424–1433.

41 W. Zhu, J. Xu, Y. Ge, H. Cao, X. Ge, J. Luo, J. Xue, H. Yang, S. Zhang and J. Cao, Epigallocatechin-3-gallate (EGCG) protects skin cells from ionizing Radiation via heme oxygenase-1 (HO-1) overexpression, *J. Radiat. Res.*, 2014, **55**, 1056–1065.

42 I. N. Zelko, T. J. Mariani and R. J. Folz, Superoxide dismutase multigene family: A comparison of the CuZn-SOD (SOD1), Mn-SOD (SOD2), and EC-SOD (SOD3) gene structures, evolution, and expression, *Free Radicals Biol. Med.*, 2002, **33**, 337–349.

43 J. Oyama, A. Shiraki, T. Nishikido, T. Maeda, H. Komoda, T. Shimizu, N. Makino and K. Node, EGCG, a green tea catechin, attenuates the progression of heart failure induced by the heart/muscle-specific deletion of MnSOD in mice, *J. Cardiol.*, 2017, **69**, 417–427.

44 J. Xiang, C. Wan, R. Guo and D. Guo, Is hydrogen peroxide a suitable apoptosis inducer for all cell types?, *Biomed Res. Int.*, 2016, **2016**, 7343965.